J|A|C|S
ARTICLES
Published on Web 04/25/2006

Site-Saturated Mutagenesis of Histidine 234 of *Saccharomyces cerevisiae* Oxidosqualene-Lanosterol Cyclase Demonstrates Dual Functions in Cyclization and Rearrangement Reactions

Tung-Kung Wu,* Yuan-Ting Liu, Cheng-Hsiang Chang, Mei-Ting Yu, and Hisng-Ju Wang

Contribution from the Department of Biological Science and Technology, National Chiao Tung University, 300, Hsin-Chu, Taiwan (Republic of China)

Received December 27, 2005; E-mail: tkwmll@mail.nctu.edu.tw

Abstract: Site-saturated mutagenesis experiments were carried out on the His234 residue of *Saccharomyces cerevisiae* oxidosqualene-lanosterol cyclase (ERG7) to characterize its functional role in ERG7 activity and to determine its effect on the oxidosqualene cyclization/rearrangement reaction. Two novel intermediates, (13α*H*)-isomalabarica-14(26),17*E*,21-trien-3β-ol and protosta-20,24-dien-3β-ol, isolated from ERG7^{H234X} mutants, provided direct mechanistic evidence for formation of the chair-boat 6−6−5 tricyclic Markovnikov cation and protosteryl cation that were assigned provisionally to the ERG7-catalyzed biosynthetic pathway. In addition, we obtained mutants that showed a complete change in product specificity from lanosterol formation to either protosta-12,24-dien-3β-ol or parkeol production. Finally, the repeated observation of multiple abortive and/or alternative cyclization/arrangement products from various ERG7^{H234X} mutants demonstrated the catalytic plasticity of the enzyme. Specifically, subtle changes in the active site affect both the stability of the cation−π interaction and generate product diversity.

Introduction

The enzymatic conversion of acyclic (3*S*)-2,3-oxidosqualene (OS) into polycyclic sterols and triterpenoids, which is catalyzed by oxidosqualene cyclases, involves a highly diverse and complex process of cyclization, rearrangement, and deprotonation steps. Over 100 distinct triterpenoid skeletons, with the $C_{30}H_{50}O$ formula, mainly form tetracycles and pentacycles. Less frequently, monocyclic, bicyclic, tricyclic, and hexacyclic triterpenoids have been isolated from various sources.[1−3,4] The diverse product profile is mainly controlled by the preorganized substrate conformation, as well as interactions between the cationic intermediate for deprotonation and the functional groups of the catalytic amino acid residues of the enzyme. In fungi and mammals, oxidosqualene-lanosterol cyclase (ERG7, EC 5.4.99.7) is proposed to bind OS in a chair−boat−chair (C−B−C) substrate conformation and initiate cyclization via the protonation of oxirane oxygen, by a conserved aspartic acid residue. This reaction propagates cyclization which will form a protosteryl cation, followed by the 1,2-shifts of the hydride and methyl groups to the lanosteryl C-8 cation. Final deprotonation occurs through abstracting a proton, either at the original C-9 site or after a hydride shift from C-9 to C-8 to form lanosterol.

Recent structure−reactivity studies of ERG7, via X-ray crystallographic analyses coupled with bioorganic and mutational data, have provided deeper insight into the catalytic cyclization/rearrangement reaction mechanism, diverse product profiles, and functional role of specific residues.[4−14] However, the functional role of a particularly interesting histidine residue, located at the 232 position of human OSC and corresponding to the 234 position of *Saccharomyces cerevisiae* ERG7, remains ambiguous. For example, Corey performed substrate-analogue labeling experiments on *S. cerevisiae* ERG7 and obtained several labeled substrates covalently attached around the His234 position (Scheme 1). This suggested that the residue may act to stabilize the reaction intermediates.[7] Thoma et al. suggested, based on the X-ray structure of human OSC, that the His232 and Phe696 residues were spatially positioned in order to stabilize the anti-Markovnikov secondary cation, which is generated at the C-14 position during the C-ring formation, through π interactions.[11] The same residue was also suggested

(1) Abe, I.; Rohmer, M.; Prestwich, G. D. *Chem. Rev.* **1993**, *93*, 2189−2206.
(2) Wendt, K. U.; Schulz, G. E.; Corey, E. J.; Liu, D. R. *Angew. Chem., Int. Ed.* **2000**, *39*, 2812−2833.
(3) Xu, R.; Fazio, G. C.; Matsuda, S. P. T. *Phytochemistry* **2004**, *65*, 261−291.
(4) Wu, T. K.; Liu, Y. T.; Chang, C. H. *ChemBioChem* **2005**, *6*, 1177−1181 and references therein.
(5) Corey, E. J.; Virgil, S. C. *J. Am. Chem. Soc.* **1991**, *113*, 4025−4026.
(6) Corey, E. J.; Virgil, S. C.; Cheng, H.; Baker, C. H.; Matsuda, S. P. T.; Singh, V.; Sarshar, S. *J. Am. Chem. Soc.* **1995**, *117*, 11819−11820.
(7) Corey, E. J.; Cheng, H.; Baker, C. H.; Matsuda, S. P. T.; Li, D.; Song, X. *J. Am. Chem. Soc.* **1997**, *119*, 1289−1296.
(8) Hart, E. A.; Hua, L.; Darr, L. B.; Wilson, W. K.; Pang, J.; Matsuda, S. P. T. *J. Am. Chem. Soc.* **1999**, *121*, 9887−9888.
(9) Joubert, B. M.; Hua, L.; Matsuda, S. P. T. *Org. Lett.* **2000**, *2*, 339−341.
(10) Meyer, M. M.; Segura, M. J. R.; Wilson, W. K.; Matsuda, S. P. T. *Angew. Chem., Int. Ed.* **2000**, *39*, 4090−4092.
(11) Thoma, R.; Schulz-Gasch, T.; D'Arcy, B.; Benz, J.; Aebi, J.; Dehmlow, H.; Hennig, M.; Stihle, M.; Ruf, A. *Nature* **2004**, *432*, 118−122.
(12) Lodeiro, S.; Segura, M. J.; Stahl, M.; Schulz-Gasch, T.; Matsuda, S. P. T. *ChemBioChem* **2004**, *5*, 1581−1585.
(13) Wu, T. K.; Chang, C. H. *ChemBioChem* **2004**, *5*, 1712−1715.
(14) Wu, T. K.; Yu, M. T.; Liu, Y. T.; Chang, C. H.; Wang, H. J.; Diau, E. W. G. *Org. Lett.* **2006**, *8*, 1319−1322.

10.1021/ja058782p CCC: $33.50

Scheme 1. Incubation of 20-Oxa-oxidosqualene with Sterol-Free *S. cerevisiae* Microsomal Protein Resulted in Isolation of a Protostane Derivative and Characterization of a Covalently Attached (*) Peptide Fragment Product near His234[7]

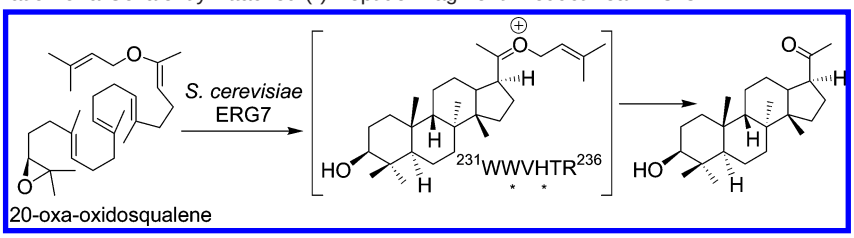

to act as a base that deprotonates to form lanosterol or may function as part of a catalytic base dyad that will influence deprotonation, via a hydrogen-bonding network, to the hydroxyl group of Tyr503. We previously performed site-directed mutagenesis experiments on the His234 residue of ERG7 to determine its catalytic activity and product profile.[4] The results showed that the ERG7^{H234Y} mutant is viable, indicating it is functional, and produces multiple triterpenes, including monocyclic achilleol A, truncated rearranged protosta-12,24-dien-3β-ol, lanosterol, and parkeol. This suggests that His234 of ERG7 can play a key role in the following processes: stabilizing various carbocationic intermediates and guiding deprotonation reactions. In addition, His234 of ERG7 can assist in generating product diversity, indicating that it has functions beyond acting as the catalytic base. The combination of these findings suggests a more complex interaction between the amino acid functional group at the His234 position and cationic intermediates and provokes further investigation into the effects of substitution of other amino acids on the catalytic activity and product profile of the cyclase.

A "site-saturated mutagenesis" approach is the replacement of the target residue with each of the other proteinogenic amino acids. This technique was applied to obtain a detailed understanding of the effects, either steric or electrostatic, of other amino acids, substituted at the His234 position. The following are features of the mutant enzymes: the enzyme conformation, the cation$-\pi$ interactions between the carbocationic intermediate and side chain functional group, and the product profile. Two novel intermediates, (13α*H*)-isomalabarica-14(26),17*E*,21-trien-3β-ol and protosta-20,24-dien-3β-ol, were isolated, for the first time, from the ERG7 mutants. These products correspond to truncation of the cyclization/rearrangement cascade, precisely at two previously proposed and long-sought stages, the C$-$B 6$-$6$-$5 tricyclic cation and protosteryl cation, respectively. Previous work by Corey et al. using ERG7 in substrate-analogue affinity labeling experiments generated trapped products, implicating these cations as intermediates, and our work here demonstrates directly that they are.[5$-$7] Mutants with 100% altered product specificity that produce either protosta-12,24-dien-3β-ol or parkeol instead of lanosterol were also obtained. Taken together, these results further support the hypothesis that diversity in product specificities could be obtained through a subtle change of the shape of the active site and/or by repositioning of crucial functional groups throughout the course of evolution.[15$-$18]

Experimental Section

Generation of Mutants. Mutagenesis of His234 in the wild type *ERG7* gene was performed using the QuickChange site-directed mutagenesis kit (Stratagene Inc., La Jolla, CA). The oligonucleotide primers used were the following, with substitutions underlined and silent mutation italicized: ERG7H234X-Degenerate1: 5′-d(TGGGTTNNS-A*CTCGAG*GTGTTTACATT)-3′; ERG7H234X-Degenerate2: 5′-d(AAT-GTAAACAC*CTCGAG*TSNNAACCCA)-3′. Mutations were confirmed by DNA sequencing using the dideoxy chain-termination method and the ABI PRISM 3100 autosequencer (Applied Biosystem, Foster City, CA). The recombinant plasmids were electroporated into the yeast strain TKW14, selected for growth on SD+Ade+Lys+His+Met+Ura+hemin+G418+Erg plates, and then reselected on SD+Ade+Lys+His+Met+Ura+hemin+G418+5-FOA plates, to determine whether the ERG7 mutant protein could complement the cyclase deficiency of TKW14, as described previously.[4,13] Transformants were grown in SD+Ade+Lys+His+Ura+Met+Hemin+Erg medium for nonsaponifiable lipid extraction and column chromatography.

Analysis of Extracts from Mutants. The extracts were fractionated by silica gel column chromatography using a 19:1 hexane/ethyl acetate mixture in order to obtain products that migrated between the following: oxidosqualene and lanosterol, lanosterol-positioned, and lanosterol and ergosterol compounds. The fractions were assayed by gas chromatography$-$mass spectrometry (GC$-$MS) and examined for triterpenoid products with a molecular mass of $m/z = 426$. The products with $m/z = 426$ were acetylated and isolated by $AgNO_3$-impregnated silica gel chromatography using 15% diethyl ether in hexane, as previously described.[19$-$21] Products were identified using 600 MHz nuclear magnetic resonance (NMR) and GC$-$MS analyses. GC$-$MS was performed on an Agilent 6890N chromatograph equipped with a DB-5HT column (30 m $\times$ 0.25 mm I.D., 0.1 μm film; oven gradient at 50 °C for 1 min, and then 10 °C per min until 300 °C, held at 300 °C for 8 min, 250 °C inlet; splitless, flow rate 1 mL/min).

Molecular Modeling. Molecular-modeling studies were performed, using the Insight II Homology program with the X-ray structure of lanosterol-complexed human OSC as the template.[11] The MODELER program is designed to extract spatial constraints such as stereochemistry, main-chain and side-chain conformation, distance, and dihedral angle from the template structure. The resulting structure was optimized using an objective function that included spatial constraints and a CHARMM energy function. The objective function combines free energy perturbation, correlation analysis, and combined quantum and molecular mechanics (QM/MM) to obtain a better description of molecular-level structure, interactions, and energetics. The homologous model structure, with the lowest objective function, was evaluated further using the Align2D algorithm for sequence-structure alignment.[22,23]

Chemical Shifts of Protosta-20,24-dien-3β-ol: Chemical shifts were referenced to $Si(CH_3)_4$ and are generally accurate to +0.01 ppm.

(15) Ourisson, G. *Pure Appl. Chem.* **1989**, *61*, 345$-$348.
(16) Corey, E. J.; Matsuda, S. P.; Bartel, B. *Proc. Natl. Acad. Sci. U.S.A.* **1993**, *90*, 11628$-$11632.
(17) Buntel, C. J.; Griffin, J. H. In *Isopentenoids and Other Natural Products: Evolution of sterol and triterpene cyclases*; Nes, W. D., Ed.; ACS Symposium Series 562; American Chemical Society: Washington, DC, 1994; pp 44$-$54.
(18) Kushiro, T.; Shibuya, M.; Ebizuka, Y. *Eur. J. Biochem.* **1998**, *256*, 238$-$244.
(19) Freimund, S.; Kopper, S. *Carbohydr. Res.* **2004**, *339*, 217$-$220.
(20) Vroman, H. E.; Cohen, A. F. *J. Lipid Res.* **1967**, *8*, 150$-$152.
(21) Pascal, R. A. J.; Farris, C. L.; Schroepfer, G. J. J. *Anal. Biochem.* **1980**, *101*, 15$-$22.
(22) Sali, A.; Blundell, T. L. *J. Mol. Biol.* **1990**, *212*, 403$-$428.
(23) Sali, A.; Blundell, T. L. *J. Mol. Biol.* **1993**, *234*, 779$-$815.

^{1}H NMR (600 MHz, $CDCl_3$): δ 5.08 (m, 1H, H-24), 4.88 (s, 1H, H-21), 4.86 (s, 1H, H-21), 3.22 (dd, J = 11.7, 5.0 Hz, 1H, H-3α), 2.60 (dt, J = 9.2, 8.8 Hz, 1H, H-17α), 2.10 (m, 1H, H-22), 2.04 (m, 1H, H-23), 1.97 (d, J = 3.6 Hz, 1H, H-13α), 1.95 (m, 1H, H-22), 1.92 (m, 1H, H-7β), 1.91 (m, 1H, H-23), 1.75 (m, 2H, H-16), 1.68 (d, J = 4.6 Hz, 1H, H-2α), 1.66 (s, 3H, H-26), 1.58 (s, 3H, H-27), 1.52 (m, 1H, H-2β), 1.49 (m, 1H, H-6), 1.46 (m, 1H, H-11β), 1.44 (t, J = 14.1 Hz, H-9β), 1.43 (d, 1H, J = 10.3 Hz, H-5α), 1.42 (d, J = 3.3 Hz, 1H, H-15), 1.38 (d, J = 3.5 Hz, 1H, H-1β), 1.37 (d, J = 2 Hz, 1H, H-1α), 1.20−1.19 (m, 1H, H-11α), 1.19−1.18 (m, 1H, H-6α), 1.18−1.17 (m, 1H, H-7 α), 1.17−1.16 (m, 1H, H-15β), 1.16−1.14 (m, 2H, H-12), 1.07 (s, 3H, Me-30), 0.96 (s, 3H, Me-29), 0.87 (s, 3H, Me-19), 0.82 (s, 3H, Me-18), 0.76 (s, 3H, Me-28). ^{13}C NMR (150.77 MHz, 30 mM solution in $CDCl_3$, 25 °C) δ 16.10 (C-28), 17.48 (C-18), 17.69 (C-27), 18.57 (C-6), 21.98 (C-30), 22.38 (C-19), 23.09 (C-11), 25.14 (C-12), 25.70 (C-26), 27.30 (C-23), 27.65 (C-16), 29.08 (C-29), 29.11 (C-2), 32.88 (C-1), 33.35 (C-15), 34.81 (C-7), 36.81 (C-10), 38.62 (C-22), 39.15 (C-4), 39.95 (C-8), 43.88 (C-17), 44.52 (C-13), 45.68 (C-9), 47.66 (C-5), 50.67 (C-14), 79.33 (C-3), 108.78 (C-21), 124.36 (C-24), 131.43 (C-25), 152.04 (C-20).

Chemical Shifts of (13α*H*)-Isomalabarica-14(26),17*E*,21-trien-3*β*-ol: Chemical shifts were referenced to $Si(CH_3)_4$ and are generally accurate to +0.01 ppm. ^{1}H NMR (600 MHz, $CDCl_3$): δ 5.11−5.08 (m, 2H, H-17 and H-21), 4.84 and 4.60 (s and s, 1H and 1H, CH_2-14), 3.23 (dd, J = 11.7, 5.0 Hz, H-3α), 2.17−2.11 (m, 2H, H-16), 2.07 (d, J = 8.9 Hz, 1H, H-13α), 2.06 (m, 2H, CH_2-20), 2.04 (m, 1H, H-16), 1.98−1.94 (m, 3H, H-12β, H-15, and CH_2-19), 1.87−1.83 (m, 1H, H-15), 1.75−1.71 (m, 1H, H-2α), 1.66 (s, 3H, Me-24), 1.63−1.62 (m, 1H, H-2β), 1.61 (m, 1H, H-7β), 1.582 (s, 3H, Me-23), 1.579 (s, 3H, Me-25), 1.55 (s, 1H, H-12α), 1.54−1.51 (5H, H-5α, H-9β, H-11β, H-6α), 1.48−1.37 (m, 3H, CH_2-1, H-11α), 1.28−1.19 (m, 2H, H-6β, H-7α), 1.09 (s, 3H, Me-27), 0.96 (s, 3H, Me-29), 0.93 (s, 3H, Me-28), 0.75 (s, 3H, Me-30). ^{13}C NMR (149.90 MHz, 30 mM solution in $CDCl_3$, 25 °C) δ 15.81 (C-30), 16.01 (C-25), 17.68 (C-23), 18.55 (C-6), 20.74 (C-11), 23.11 (C-28), 25.69 (C-24), 26.53 (C-16), 26.72 (C-20), 28.36 (C-12), 29.08 (C-29), 29.17 (C-2), 29.64 (C-27), 31.93 (C-7), 34.27 (C-1), 35.27 (C-10), 39.06 (C-4), 39.22 (C-15), 39.69 (C-19), 44.79 (C-8), 46.70 (C-5), 52.31 (C-9), 56.47 (C-13), 79.53 (C-3), 109.14 (C-26), 124.15 (C-17), 124.37 (C-21), 131.29 (C-22), 135.14 (C-18), 155.08 (C-14).

Results and Discussion

Plasmids carrying the ERG7^{H234X} (with X denoting the saturated mutations) mutations were constructed by polymerase chain reaction (PCR) using two complementary synthetic oligonucleotide primers containing degenerate bases at the His234 position. The constructs were analyzed to determine whether they could support viability of a HEM1 and ERG7 double-knockout *S. cerevisiae* strain, TKW14, that is only viable when supplied with exogenous ergosterol.[4,13,24] Wild-type ERG7 expressed from a plasmid supports growth of TKW14 in the absence of exogenous ergosterol.[13] Next, the product profiles generated by the ERG7 mutant enzymes (in a strain expressing the mutant enzyme as the oxidosqualene cyclase) were analyzed. Strains grown in liquid media were harvested, and nonsaponifiable lipid (NSL) extracts were prepared. Products were separated using $AgNO_3$-impregnated silica gel columns, and those with a molecular mass of m/z = 426 were characterized using GC−MS and NMR.

The ERG7^{H234X} mutants showed diverse profiles of products with a molecular mass of m/z = 426. Four product compounds were indistinguishable from authentic achilleol A, protosta-12,-24-dien-3β-ol, lanosterol, and parkeol standards by ^{1}H and ^{13}C NMR, as well as GC−MS. A fifth compound migrating on the GC column with a retention time of 0.25 min relative to parkeol was isolated and demonstrated to be protosta-20,24-dien-3β-ol based on the following data. The compound showed a distinct ^{1}H NMR chemical shift with one olefinic proton (δ 5.08) and two methylene protons (δ 4.88, 4.86), as well as seven methyl singlets (δ 1.66, 1.58, 1.07, 0.96, 0.87, 0.82, and 0.76). The 150 MHz ^{13}C NMR spectrum revealed the presence of one secondary-quaternary and one tertiary-quaternary substituted double bond (δ = 108.78, 152.04 and 124.36, 131.43 ppm). The latter is characteristic of a double bond at the hydrocarbon side chain. The HSQC spectrum showed that the olefinic methylene protons at δ 4.88 and 4.86 are attached to the carbon at 108.78 ppm, while the methine proton at δ 2.60 is attached to the carbon at 43.88 ppm (C-17). In the ^{1}H−^{1}H COSY spectrum, the methine proton at δ 2.60 shows connectivity with the two olefinic methylene protons at δ 1.75 and the methine proton at δ 1.97, which are attached to carbons at 27.65 ppm (C-16) and 44.52 ppm (C-13), respectively. In the HMBC spectrum, the δ 2.60 methine proton is coupled by ^2J to carbons at 152.04 ppm (C-20), 27.65 ppm (C-16), and 44.52 ppm (C-13). The δ 2.60 methine proton is coupled by ^3J connectivity to a carbon at 108.78 ppm (C-21), as well as to 38.62 (C-22) and 50.67 ppm (C-14). The HMBC also established that the tertiary vinylic proton (δ 5.08) is coupled by ^2J to carbons at 27.30 (C-23) and 131.43 ppm (C-25), as well as by ^3J connectivity to carbons at 38.62 ppm (C-22), 17.69 ppm (C-27), and 25.70 ppm (C-26). Additional HSQC and HMBC correlations showed ^3J connectivity between olefinic methylene protons (δ 4.88 and 4.86) and carbons at 38.62 ppm (C-22) and 43.88 ppm (C-17). These correlations unambiguously establish key structural features of the two double bonds located between C-20 and C-21, and C-24 and C-25, respectively. Finally, the presence of NOEs among Me-19/Me-28, Me-18/H-21, Me-18/H-9, Me-19/H-9, Me-29/H-3, and H-3/H-5, as well as the absence of NOEs among Me-19/Me-30, Me-18/Me-30, and Me-18/H-17, confirm the structure to be protosta-20,24-dien-3β-ol, a product with $\Delta^{20,24}$ double bonds and a C-17β hydrocarbon side chain configuration (Figure 1A). This is the first reported isolation of this product derived from the protosteryl cation without rearrangement of the C-17α hydride.

A sixth distinct product isolated from the ERG7^{H234L}, ERG7^{H234M}, ERG7^{H234D}, and ERG7^{H234N} mutants was determined to be (13α*H*)-isomalabarica-14(26),17*E*,21-trien-3β-ol, a chair−boat (C−B) 6−6−5 tricyclic product with trans−syn−trans stereochemistry and $\Delta^{14(26),17,21}$ double bonds. Confirmation of the structure, including the stereochemistry and connectivity of C-8 and C-13, was obtained by analyzing the following NMR and MS spectroscopic data. First, the EI low mass spectrum showed a molecular ion at m/z = 426 and fragment peaks at 357, 339, 289, and 247, corresponding to the molecular formula $C_{30}H_{50}O$ ($[M]^+$), $[M - C_5H_9]^+$, $[M - C_5H_9 - H_2O]^+$, $[M - C_{10}H_{17}]^+$, and $[M - C_{13}H_{21} - H_2]^+$, respectively. Further, the ^{1}H NMR showed signals of seven methyl singlets (δ 1.66, 1.582, 1.579, 1.09, 0.96, 0.93, 0.75), two singlets of double bond protons (δ 4.84, 4.60), and two multiplet double bond protons (δ 5.11−5.08). These NMR results indicate the presence of two hydrocarbon side chain double bonds and one exocyclic double

(24) Shi, Z.; Buntel, C. J.; Griffin, J. H. *Proc. Natl. Acad. Sci. U.S.A.* **1994**, *91*, 7370−7374.

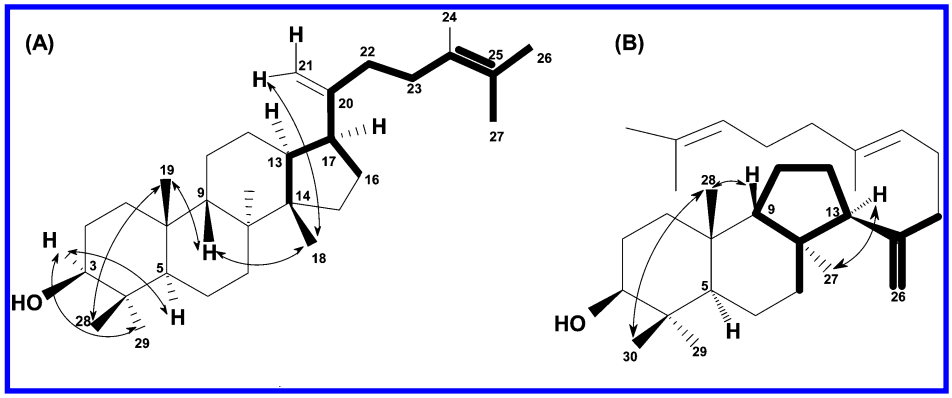

Figure 1. Bond connectivity and stereochemistry established by HMBC/HSQC (−) and NOEs (↔) spectra of (A) protosta-20,24-dien-3β-ol and (B) (13α*H*)-isomalabarica-14(26),17*E*,21-trien-3β-ol.

Table 1. Product Profile of *S. cerevisiae* TKW14 Expressing the ERG7^{H234X} Site-Saturated Mutants

amino acids substitution	product profile						
	no products	achilleol A	iso-malabarica-14(26),17,21-trien-3β-ol	protosta-12,24-dien-3β-ol	protosta-20,24-dien-3β-ol	lanosterol	parkeol
Gly				29	7	17	47
Ala				17	13	30	40
Val						42	58
Leu			30			39	31
Ile						70	30
Pro						64	36
Cys				7	4	67	22
Met		17	10			31	42
Asn			26	23	14	27	10
Gln						100	
Ser				100			
Thr							100
Tyr		14		26		51	9
Phe		66				14	20
Trp							100
Lys	V						
Arg	V						
His						100	
Asp			58			30	12
Glu						49	51

bond. The ^{13}C NMR also showed the presence of two tertiary-quaternary and one secondary-quaternary substituted double bonds (δ = 124.37, 131.29 and 124.15, 135.14, as well as 109.14, 155.08 ppm), which are similar to those of the tricyclic nucleus. Furthermore, the HSQC spectrum established that the double bond protons at δ 4.84 and 4.60 are attached to the carbon at 109.14 ppm (C-26) and that the methine proton at δ 2.07 is attached to the carbon at 56.47 ppm (C-13). In the HMBC spectrum, the δ 2.07 methine proton is coupled by ^2J to carbons at 155.08 ppm (C-14), 44.79 ppm (C-8), and 28.36 ppm (C-12), as well as by ^3J to carbons at 109.14 ppm (C-26), 52.31 ppm (C-9), 39.22 ppm (C-15), 31.93 ppm (C-7), 29.64 ppm (C-27), and 20.74 ppm (C-11), thus establishing connectivity of the germinal protons on the double bond adjacent to a tricyclic nucleus. Finally, the presence of NOEs between Me-28/Me-30, Me-27/H-13, and Me-28/H-9, as well as the absence of NOEs between Me-27/Me-28, Me-27/H-9, Me-28/H-5, and H-9/H-13, were uniquely consistent with the stereochemistry of the C−B 6−6−5 tricyclic nucleus. These findings unambiguously establish the structure to be (13α*H*)-isomalabarica-14(26),17*E*,21-trien-3β-ol, which is a tricyclic abortive cyclization product with $\Delta^{14(26),17,21}$ double bonds and trans−syn−trans stereochemistry on the 6−6−5 tricyclic nucleus (Figure 1B). Interestingly, Corey and co-workers incubated the 20-oxa analogue of oxidosqualene, with the sterol-free microsomal protein of *S. cerevisiae*, which resulted in the isolation of two truncated products, a 17β-acetylprotostane derivative and an isomeric tetracyclic compound, structurally similar to the protosta-20,24-dien-3β-ol and (13α*H*)-isomalabarica-14(26),-17*E*,21-trien-3β-ol.[5,6] The absolute configuration of (13α*H*)-isomalabarica-14(26),17*E*,21-trien-3β-ol was not determined directly within the lanosterol biosynthetic pathway but had been provisionally assigned based on biosynthetic evidence. Thus, this work describes the first intermediate of the oxidosqualene cyclization/rearrangement cascade that is derived from the direct trapping of the C−B 6−6−5 Markovnikov tricyclic cation.

The product profiles of each mutant are summarized in Table 1. Several mutants including ERG7^{H234M}, ERG7^{H234L}, and ERG7^{H234D} produced (13α*H*)-isomalabarica-14(26),17*E*,21-trien-3β-ol as part of the product profile. The ERG7^{H234G}, ERG7^{H234A}, and ERG7^{H234C} mutants produced protosta-20,24-dien-3β-ol, in addition to other products. Interestingly, the ERG7^{H234N} mutant simultaneously produced (13α*H*)-isomalabarica-14(26),17*E*,21-trien-3β-ol, protosta-20,24-dien-3β-ol, protosta-12,24-dien-3β-ol, lanosterol, and parkeol, but not monocyclic achilleol A. In contrast, the ERG7^{H234S} mutant produced a minor amount of protosta-12,24-dien-3β-ol as the sole product. The ERG7^{H234Q} mutant produced lanosterol as the sole product. Finally, the ERG7^{H234T} and ERG7^{H234W} mutants produced minor amounts of parkeol as the sole product.

Scheme 2. Proposed Cyclization/Rearrangement Pathways of Oxidosqualene in *S. cerevisiae* TKW14 Expressing ERG7^{H234X} Site-Saturated Mutations

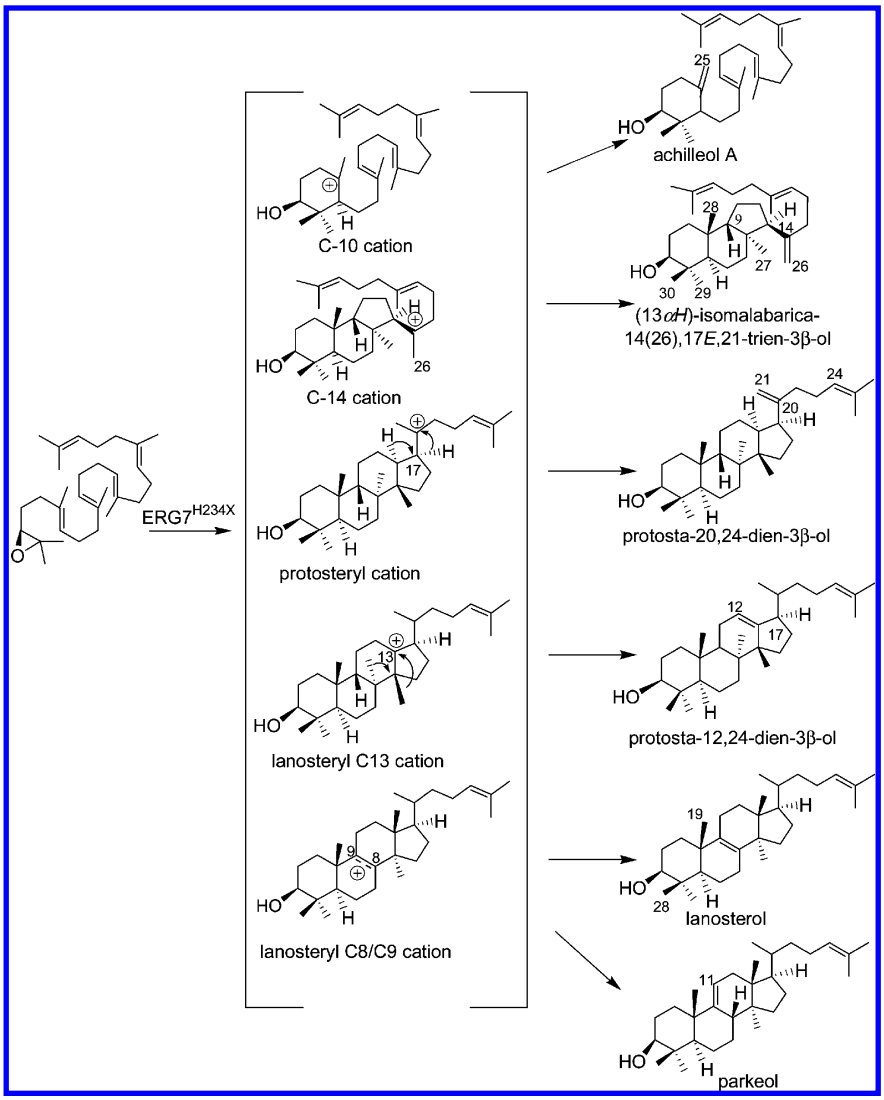

As shown in Scheme 2, protonation of the epoxide group of prefolded OS initiates opening of the oxirane ring and A-ring cyclization to a monocyclic C-10 cation (lanosterol numbering). This is followed by deprotonation from Me-25, resulting in the production of achilleol A.[25] Further cyclization of the B- and C-ring proceeds, via a chair−boat conformation and a Markovnikov-favored 6−6−5 ring closure, to produce a tricyclic C-14 cation that directly abstracts the C-26 proton, yielding (13α*H*)-isomalabarica-14(26),17*E*,21-trien-3*β*-ol. C-ring expansion from the tertiary cyclopentylcarbinyl cation leads to anti-Markovnikov secondary cyclohexyl carbocation, followed by D-ring annulation to generate the protosteryl C-20 cation, a tetracyclic carbocation with the natural C-20*R* configuration and C-17*β* side chain. Direct deprotonation of the protosteryl cation at C-21 generates protosta-20,24-dien-3*β*-ol as the end product. Alternatively, a backbone rearrangement of H-17α→20α and H-13α→17α, via 1,2-hydride shifts, generates the C-13 cation that, when combined with elimination of H-12, yields protosta-12,24-dien-3*β*-ol with a Δ^{12} double bond. Finally, skeletal rearrangement involving two additional methyl-group shifts (Me-14*β*→Me-13*β* and Me-8α→Me-14α) and a hydride shift from H-9*β* to H-8*β* generates the lanosteryl C-9 cation that undergoes deprotonation at C-8 and C-11 to form the sterol precursors, lanosterol and parkeol, respectively.

The lack of a high-resolution crystal structure of *S. cerevisiae* wild-type and mutated ERG7 proteins when bound to substrate or product makes it difficult to determine how ERG7^{H234X} saturated mutants generate multiple product profiles.[25,26] To determine how the ERG7^{H234X} mutants differentially affect deprotonation positions and generate multiple product profiles, we used a homology model derived from the human OSC X-ray crystal structure (Figure 2). Using this model, the template and homology modeled structures showed good accordance of secondary structure and 3-D profile, as previously described.[4,11,13,14] The homology model of ERG7 showed that the His234 hydrogen bonds connect with Tyr510 and are spatially near the C-13 and C-20 positions of lanosterol. The *π*-electron-rich pocket of His234 is also optimal to stabilize the electron-deficient cationic intermediate. Simulated substitution of ERG7^{H234} with other amino acid residues showed that this position affects steric or electrostatic interactions between the cationic intermediate and the active site residue side chain. For

(25) Wendt, K. U. *Angew. Chem., Int. Ed.* **2005**, *44*, 3966−3971.

(26) Rajamani, R.; Gao, J. *J. Am. Chem. Soc.* **2003**, *125*, 12768−12781.

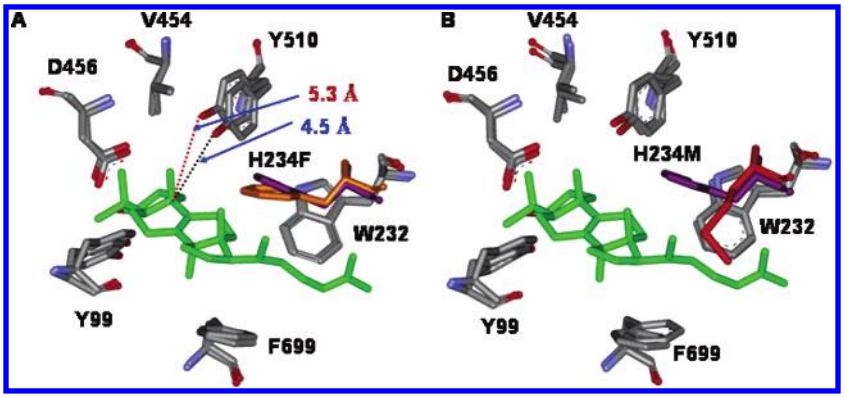

Figure 2. Superposition of the *S. cerevisiae* ERG7^{H234} wild-type (violet) with (A) ERG7^{H234F} (orange) and (B) ERG7^{H234M} (blue) mutants. The black and red dotted lines show interactions of the C-9 lanosterol cation (green) with the phenolic oxygen of Tyr510 in the wild-type and ERG7^{H234F} mutant, respectively.

example, substitution of His234 with small nonpolar hydrophobic residues enlarged the distance between the amino acid side chain and the cationic intermediate near positions C-13 and C-20. This, in turn, facilitated the production of parkeol, protosta-12,24-dien-3β-ol, and protosta-20,24-dien-3β-ol but interfered with achilleol A formation. Consistent with this observation is the increased production of parkeol and decreased production of protosta-12,24-dien-3β-ol and protosta-20,24-dien-3β-ol, when larger side chains, such as Val or Ile, were substituted for His234. Similarly, substitution of His234 with Tyr introduced both steric hindrance and electrostatic repulsion to Tyr510, causing relocation of the potential proton acceptors and forming both monocyclic and altered rearrangement products.[4] The simulation of ERG7^{H234F} showed an increased distance between hydroxyl group of Tyr510 and C-9 cation of the lanosterol of ~0.8 Å, changing from 4.5 Å to about 5.3 Å. In addition, the Tyr510 side chain shifted slightly out of the active site cavity, allowing more achilleol A formation while blocking protosta-20,24-dien-3β-ol production. Similarly, steric and electronic effects were also observed with ERG7^{H234S}, ERG7^{H234T}, and ERG7^{H234W} mutants, resulting in an altered product profile from lanosterol to protosta-12,24-dien-3β-ol and parkeol, respectively. As shown in Figure 2B, an altered side chain orientation in the ERG7^{H234M} mutant compromises the cation$-\pi$ interaction between the intermediate carbocation and Phe699, resulting in destabilization of the Markovnikov tertiary cation created at C-14 during the C-ring formation, and consequently facilitates formation of (13α*H*)-isomalabarica-14(26),17*E*,21-trien-3β-ol.[11] However, the possibility that mutation at His234 opens a new cyclization pathway leading to the Markovnikov C−B 6−6−5 cation and subsequent formation of (13α*H*)-isomalabarica-14(26),17*E*,21-trien-3β-ol cannot be excluded at the moment.

These experiments illustrate how subtle changes in the ERG7^{H234} catalytic environment have electronic effects on the intrinsic His234:Tyr510 H-bonding network and/or sterically alter the active site cavity structure. Consequently, different interactions with the reaction intermediate or neighboring amino acid residues are produced, yielding diverse product profiles. Production of products with stringent specificity could be obtained by a single amino acid substitution at the His234 position of ERG7. On the other hand, the repeated observation of multiple triterpene products from various ERG7^{H234X} mutants demonstrates the difficulty in separating steric effects from electrostatic interactions, when determining product specificity. In parallel, isolation of (13α*H*)-isomalabarica-14(26),17*E*,21-trien-3β-ol and protosta-20,24-dien-3β-ol provides long-sought support for the hypothesis that formation of lanosterol from oxidosqualene in ERG7-catalyzed cyclization/rearrangement reactions proceeds via the Markovnikov C−B 6−6−5 tricyclic cation. The subsequent protosteryl cation, with the novel C-17β hydrocarbon side chain intermediate, then undergoes rearrangement and deprotonation. Further studies should focus on elucidating the precise molecular interactions involved in the chair−boat bicyclic intermediate conformation and the required rearrangements of 1,2-hydride and methyl groups to form lanosterol.

Acknowledgment. We thank the National Chiao Tung University and the National Science Council of the Republic of China for financial support of this research under Contract No. NSC-93-2113-M-009-012. We are grateful to Ms. Chu-Lan Peng (National Tsing-Hua University) for performing the NMR spectra and to Dr. John H. Griffin and Prof. Tahsin J. Chow for helpful advice.

Supporting Information Available: Characterization of (13α*H*)-isomalabarica-14(26),17*E*,21-trien-3β-ol and protosta-20,24-dien-3β-ol are described. This material is available free of charge via the Internet at http://pubs.acs.org.

JA058782P